LETTER

Local generation of glia is a major astrocyte source in postnatal cortex

Woo-Ping Ge[1], Atsushi Miyawaki[2], Fred H. Gage[3], Yuh Nung Jan[1] & Lily Yeh Jan[1]

Glial cells constitute nearly 50% of the cells in the human brain[1]. Astrocytes, which make up the largest glial population, are crucial to the regulation of synaptic connectivity during postnatal development[2]. Because defects in astrocyte generation are associated with severe neurological disorders such as brain tumours[3], it is important to understand how astrocytes are produced. Astrocytes reportedly arise from two sources[4–6]: radial glia in the ventricular zone and progenitors in the subventricular zone, with the contribution from each region shifting with time. During the first three weeks of postnatal development, the glial cell population, which contains predominantly astrocytes, expands 6–8-fold in the rodent brain[7]. Little is known about the mechanisms underlying this expansion. Here we show that a major source of glia in the postnatal cortex in mice is the local proliferation of differentiated astrocytes. Unlike glial progenitors in the subventricular zone, differentiated astrocytes undergo symmetric division, and their progeny integrate functionally into the existing glial network as mature astrocytes that form endfeet with blood vessels, couple electrically to neighbouring astrocytes, and take up glutamate after neuronal activity.

Most radial glia have finished producing their share of astrocytes and have begun to disappear shortly after birth[4–6]; astrocytes are therefore thought to derive mainly from progenitors in the subventricular zone (SVZ) at later stages[8]. The massive expansion of glia within the first three postnatal weeks presents a daunting task for their presumed SVZ progenitors. This task is rendered even more challenging by the thickening of the cortex compounded by the disappearance of radial glia, which provides the migratory tracks for newly formed astrocytes[9]. We used electroporation to transfect green fluorescent protein (GFP) plasmids into SVZ/radial glial cells of mice at postnatal days (P)0–2 to label them with GFP *in vivo* and to trace their progeny at P16–20 (Fig. 1a and Supplementary Fig. 1). Only a very small percentage (about 3%) of the astrocytes derived postnatally from SVZ/radial glial cells reached cortical layers I–IV; most were left behind in SVZ/white matter (75%) and layers V–VI (22%) (Fig. 1b, c). It therefore seems that huge numbers of cortical astrocytes generated postnatally might arise from a more efficient process, such as local cell proliferation (Ki67^{+}; Fig. 1d), rather than from SVZ progenitors. Whereas glial cell division within the cortex was reported half a century ago, on the basis of studies involving [³H]thymidine incorporation into DNA[10], the extent of the contribution of local glial division to postnatal astrocyte production remained unknown, owing to the difficulty in distinguishing glia generated locally from glia derived from other sources. In this study, we have obtained evidence to support the hypothesis that the local generation of astrocytes within the postnatal cortex is a major source of glia.

To label locally generated glia, we used a replication-defective murine leukaemia retrovirus (MLV) to express GFP in infected dividing cells and their progeny in postnatal cortex *in vivo*. This retrovirus specifically infects proliferating cells and has been used for cell-fate tracing in SVZ and the hippocampal subgranular zone (SGZ) *in vivo*[8,11]. We injected
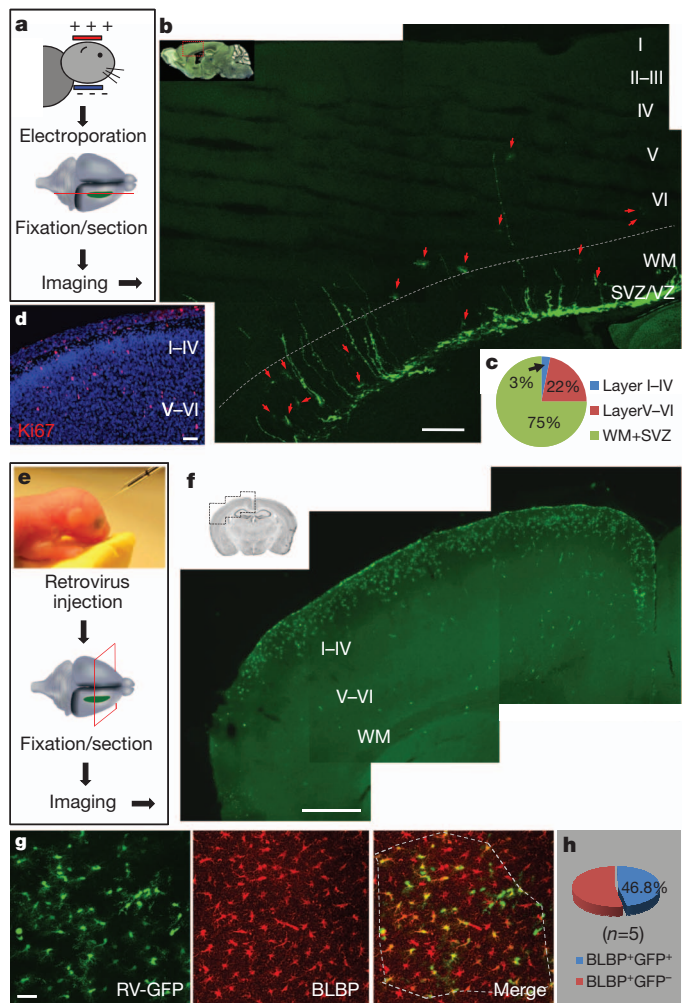
Figure 1 | Locally generated glia as a major source of astrocytes.
a, Procedure to label SVZ/radial glia-derived astrocytes by electroporation. **b**, The distribution of astrocytes (arrows) 2 weeks after electroporation. VZ, ventricular zone. **c**, Percentages of astrocytes at different locations. WM, white matter. **d**, Proliferating cells (Ki67^{+}, red) in a cortical section of P3 mouse. Nuclei were stained with 4′,6-diamidino-2-phenylindole (DAPI, blue). **e**, Procedure to label locally proliferating cells by retrovirus. **f**, Cells labelled by retrovirus (green). **g**, Image of infected astrocytes. Astrocytes (BLBP[+], red) with GFP (GFP[+]BLBP[+]) or without GFP (GFP[−]BLBP[+]) in the outlined region (dashed line) were included for analysis in **h**. RV, retrovirus. **h**, Percentages of astrocytes labelled by retrovirus injected locally, calculated as $100 \times (\text{BLBP}^+\text{GFP}^+ \text{ cells}/\text{BLBP}^+ \text{ cells})$. Scale bars, 200 μm (**b**), 50 μm (**d**), 500 μm (**f**) and 40 μm (**g**).

[1]Howard Hughes Medical Institute, Departments of Physiology, Biochemistry and Biophysics, University of California at San Francisco, 1550 4th Street, San Francisco, California 94158, USA. [2]Life Function and Dynamics, Exploratory Research for Advanced Technology, Japan Science and Technology Agency, and Brain Science Institute, RIKEN, Wako-city, Saitama, 351-0198, Japan. [3]Laboratory of Genetics, The Salk Institute for Biological Studies, La Jolla, California 92037, USA.

viruses locally into layers I–IV of the barrel or motor cortex of wild-type mice at P0–6 (Fig. 1e, f) and examined GFP expression 1 week later in samples that were also stained with antibodies against brain lipid-binding protein (BLBP) (Fig. 1g), which labels radial glia during embryonic development and astrocytes in the postnatal brain[12]. Whereas about 30% of infected cells were NG2 glia (27.6%, $n = 662$ infected cells, Supplementary Fig. 2), 55–70% of infected cells were astrocytes (BLBP$^+$, 56.9%, $n = 369$ GFP$^+$ cells, Fig. 1g; GFAP$^+$, 68.6%, $n = 662$ GFP$^+$ cells, Supplementary Fig. 2), indicating that these astrocytes originated locally *in vivo*.

To determine whether a major astrocyte source was derived from the local generation of glia, we injected retroviruses with higher titre (1 μl, (1–3) × 10^7) into the cortex of P0–2 mice and compared the number of GFP-expressing astrocytes (BLBP$^+$GFP$^+$) with the total number of astrocytes (BLBP$^+$) within an infected region 7–10 days

after injection. We found that nearly half of the astrocytes were doubly labelled (GFP$^+$BLBP$^+$, 46.8 ± 3.8%, $n = 5$ mice; Fig. 1f–h). Because the half-life of infectivity of MLV retrovirus is 5–8 h at 37 °C, the doubly labelled astrocytes probably correspond to astrocytes undergoing division in the time window of 5–8 h plus the progeny they generate over the course of 7–10 days. Control studies revealed no differences in the morphology of astrocytes (Fig. 1g), the density of dividing cells (Supplementary Fig. 3) or the percentage of GFAP-occupied area (Supplementary Fig. 4) in brain regions with or without retroviral infection. Our observations therefore suggest that local pro-liferation is a major source of astrocytes in the postnatal cortex.

To test the possibility that multiple dividing cell types infected by retroviruses, including astrocytes, NG2 glia and perhaps some unknown progenitors in the cortex, gave rise to these GFP-expressing astrocytes, we labelled acute brain slices with the nuclear marker
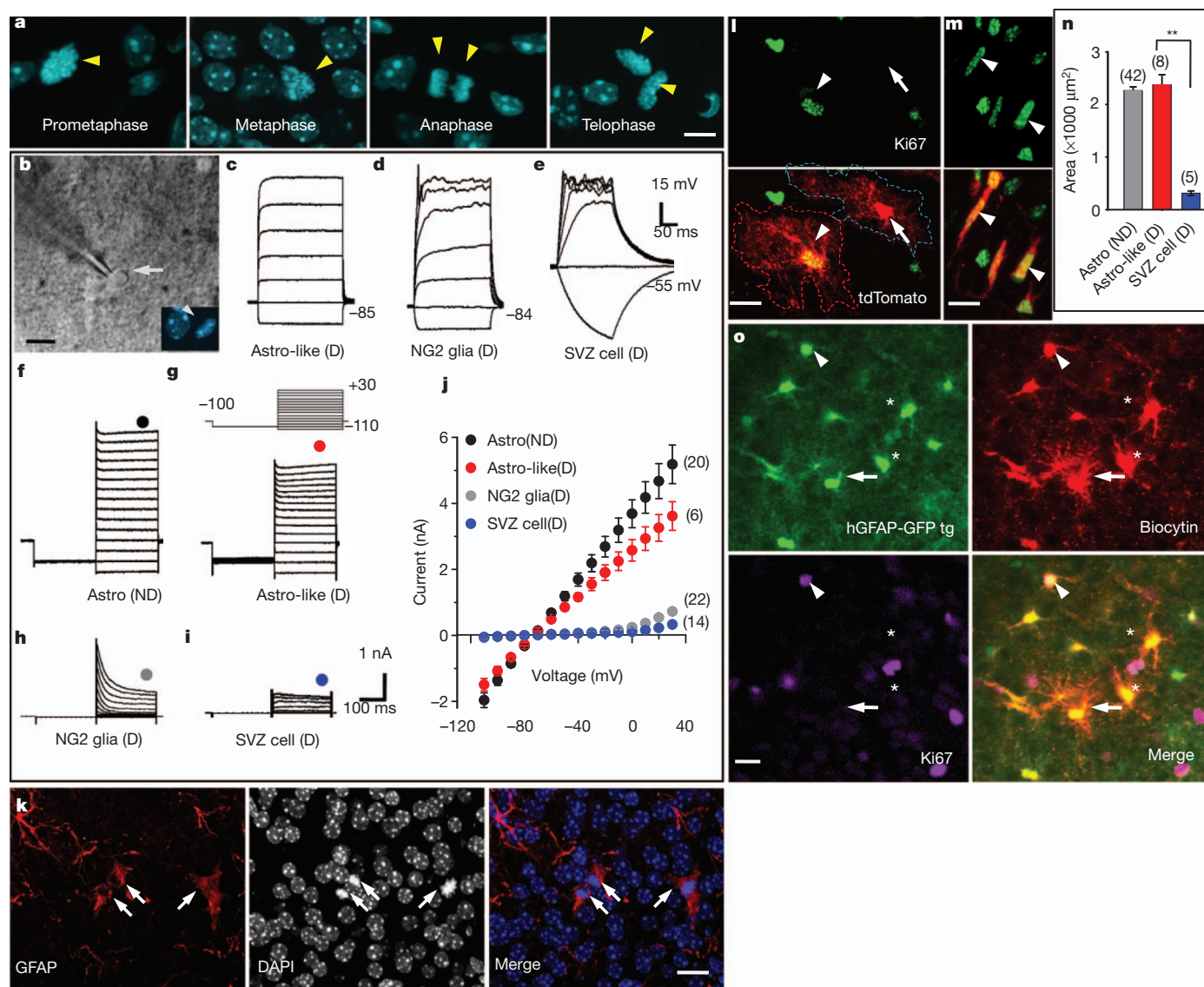
Figure 2 | Properties of dividing cells within the cortex. a, Nuclei (arrowheads, Hoechst 33342) of dividing cells at different mitotic stages in acute brain slices. **b**, A dividing cell (differential interference contrast, arrow) at prometaphase (Hoechst 33342, arrowhead). **c–e**, Voltage responses from an Astro-like-D cell (**c**), a dividing NG2 glia (**d**) and a dividing SVZ cell (**e**). **f–i**, Current responses from a non-dividing (ND) astrocyte (**f**), an Astro-like-D cell (**g**), a dividing NG2 glia (**h**) and a dividing SVZ cell (**i**) evoked by step voltages (inset, **g**). **j**, Current–voltage curves in **f–i** (the circles indicate the positions of measurements). **k**, Astro-like-D cells (arrows; two at telophase, one at metaphase) stained with anti-GFAP (red). **l, m**, Morphology of a non-dividing astrocyte (arrow) and an Astro-like-D cell (arrowhead, **l**) in the cortex, and dividing cells (arrowheads) in the SVZ (**m**) of a P8 hGFAP-CreER;Ai14 transgenic mouse. **n**, Summary of the area covered by the processes of non-dividing astrocytes (grey), Astro-like-D cells (red) and SVZ dividing cells (blue) (10-μm z-projection with soma included, one-way analysis of variance followed by a Bonferroni post-hoc test; two asterisks, $P < 0.01$). **o**, A non-dividing astrocyte (arrow) was loaded with biocytin. A dividing astrocyte is labelled by biocytin (arrowhead). tg, transgenic. Scale bars, 5 μm (**a**) and 10 μm (**b, k–m, o**). Error bars indicate s.e.m.

Hoechst 33342, a dye that can permeate live cell membranes, to distinguish dividing cells from non-dividing cells (Fig. 2a). In some experiments we also used slices from CAG-Fucci-Green transgenic mice to identify dividing cells in the SVZ and cortex (Supplementary Fig. 5). In this line, the green fluorescent protein mAG accumulates specifically during the S (synthesis) to M (mitosis) stages of the cell cycle[13], thus facilitating the identification of dividing cells for whole-cell patch-clamp recordings (Fig. 2b). Excluding cells of the vascular system, 94.6% (87 of 92 cells, P6–13) of the dividing cells in the cortex fell into two groups: dividing NG2 glia[14], with characteristic small sodium currents and rectifying current–voltage (I–V) curve (Fig. 2d, h, j) and astrocyte-like dividing cells (Astro-like-D; Fig. 2c, g, j), so named for their similarity to differentiated astrocytes (Fig. 2f, j). Astrocytes characteristically displayed large, delayed rectifier potassium currents (K_{dr}) and large, inwardly rectifying potassium currents (K_{ir}) but no sodium currents, and they had a linear I–V curve[15] (Fig. 2f, j). In contrast, dividing cells recorded in the SVZ (Supplementary Fig. 5) had no K_{ir} current and a very small K_{dr} (Fig. 2e, i, j), typical of immature progenitors[16]. To further characterize the Astro-like-D cells, our immunostaining revealed that they were GFAP$^+$ but Nestin$^-$ (Fig. 2k and Supplementary Fig. 6). We then compared the morphology of

Astro-like-D cells with that of mature astrocytes or SVZ dividing progenitors in hGFAP-CreER;Ai14 transgenic mice. Crossing Ai14 transgenic mice[17] with hGFAP-CreER transgenic mice[18] allowed robust expression of the red fluorescent protein tdTomato after inducible astrocyte-specific Cre-mediated recombination. We administered tamoxifen to hGFAP-CreER;Ai14 transgenic mice at P0–2 and assessed the cellular morphology 1 week later (Supplementary Fig. 7). Astro-like-D cells (Ki67$^+$tdTomato$^+$) had a complex morphology comparable to that of neighbouring mature astrocytes (Ki67$^-$tdTomato$^+$; Fig. 2l, n and Supplementary Fig. 8). In contrast, SVZ dividing progenitors had a bipolar/unipolar morphology (Ki67$^+$tdTomato$^+$; Fig. 2m, n and Supplementary Fig. 8). Because coupling by means of gap junctions is a hallmark feature of astrocytes, we injected biocytin into individual non-dividing astrocytes in brain slices of hGFAP-GFP transgenic mice, which express GFP under the control of human astrocyte-specific GFAP promoter[19], and found that Astro-like-D cells (Ki67$^+$GFP$^+$) and mature astrocytes (Ki67$^-$GFP$^+$; Fig. 2o) were coupled by means of gap junctions. Thus, unlike SVZ dividing progenitors (Fig. 2e, i, j) and glioblasts[20], Astro-like-D cells in the cortex are differentiated astrocytes. Taken together with a previous report[21] and our tracing results from NG2-CreBac/ER^{TM};Ai14
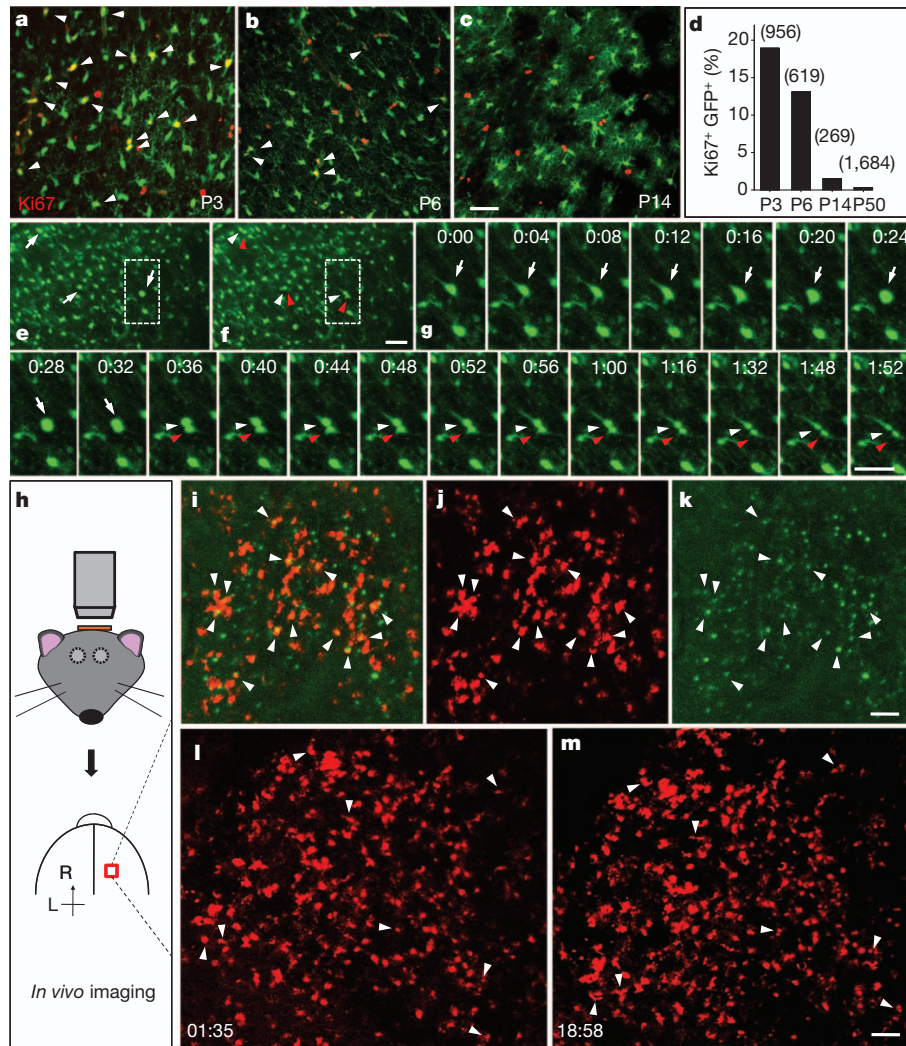
Figure 3 | Time-lapse imaging of local proliferation of astrocytes.
a–c, Proliferating astrocytes (arrowheads) in the cortex of hGFAP-GFP transgenic mice, at P3 (**a**), P6 (**b**) and P14 (**c**). **d**, Summarized data for the percentage of Ki67$^+$GFP$^+$ cells among GFP$^+$ cells with strong GFP signals. **e, f**, Sequential images of a cortical slice from a P3 hGFAP-GFP transgenic mouse (**e**, parent cells (arrows); **f**, daughter cells (arrowheads). **g**, Time-lapse images

(1 h 52 min) of a dividing GFP$^+$ cell in **e** and **f**. **h**, Procedure to image cell division *in vivo*. **i–k**, Images from a P4 triply transgenic hGFAP-CreER;Ai14;CAG-Fucci-Green mouse (**i**, combined images; **j**, tdTomato; **k**, mAG signal; arrowheads, dividing astrocytes). **l, m**, Time-lapse images at 1 h 35 min (**l**) and 18 h 58 min (**m**) from a P5 hGFAP-CreER;Ai14 transgenic mouse (arrowheads, dividing astrocytes). Scale bars, 40 μm (**a–g**) and 100 μm (**k, m**).

transgenic mice showing that NG2 glia generated very few astrocytes in the cortex during postnatal life (data not shown), our results reveal that Astro-like-D cells are the parent cells of locally generated astrocytes.

To assess the abundance of proliferating astrocytes within the cortex, we perfused hGFAP-GFP transgenic mice for Ki67 immunostaining and observed numerous astrocytes in the process of cell division before P10 (18.9% at P3, $n = 956$ GFP$^+$ cells; 13.1% at P6, $n = 619$ GFP$^+$ cells; 1.5% at P14, $n = 269$ GFP$^+$ cells; 0.30% at P48–52, $n = 1,684$ GFP$^+$ cells; Fig. 3a–d and Supplementary Fig. 9). To directly monitor local generation of astrocytes, we performed time-lapse imaging of acute cortical slices from hGFAP-GFP transgenic mice and found that roughly 2% of astrocytes divided within 3 h ($2.0 \pm 0.2\%$, 16 of 809 cells with strong GFP signals from five mice, P3–5; Fig. 3e–g and Supplementary Movie 1). Because NG2 glia maintain proliferative ability throughout life[14], and some hippocampal NG2 glia are reported to have a very weak GFP signal in another hGFAP-GFP transgenic line[22], we tested whether NG2 glia could have been among the dividing cells with a strong GFP signal, by loading biocytin into cells with a strong GFP signal through a recording pipette. We found that biocytin diffused only among cells with strong GFP signals ($n = 5$ slices; Supplementary Fig. 10), which is consistent with our observations from doubly transgenic hGFAP-GFP;NG2BacDsRed mice (Supplementary Fig. 11). Thus, the dividing cells with strong GFP expression are astrocytes rather than NG2 glia.

The density of dividing cells in acute brain slices showed no obvious change within a 6-h period after slice preparation (Supplementary Fig. 12); however, mature astrocytes could conceivably be induced to undergo local gliogenesis by means of a stab wound in vivo[23]. We therefore performed in vivo imaging with an open skull but an intact pial surface within 1 h after surgery on the triply transgenic hGFAP-CreER;Ai14;CAG-Fucci-Green mice (Fig. 3h). We observed abundant dividing astrocytes (12.4%, tdTomato$^+$mAG$^+$; Fig. 3i–k, P3–6), a similar observation to that in brain sections (Fig. 3a, b, d). Because the thinned skull preparation does not cause astrocytic gliosis or activation of microglia[24], we then performed long-term time-lapse imaging with the thinned skull preparation in hGFAP-CreER;Ai14 transgenic mice and obtained similar results: abundant astrocytes were generated locally within the cortex (about 8% of progeny, $(8 \times 2)/212$ cells in Fig. 3l, m). Because of the difficulty of identifying a dividing cell under thinned skull if its two daughter cells did not separate completely, we probably underestimated the percentage of astrocytes produced on the basis of in vivo time-lapse imaging.

To determine whether dividing astrocytes in the cortex undergo symmetric division to produce astrocytes, or asymmetric division to generate multiple cell types as SVZ cells do[8,25], we recorded from their progeny during and shortly after cytokinesis (Fig. 4a, b). The two daughter cells shared similar I–V relationships that were characteristic of astrocytes (Fig. 4c). In addition, we examined the daughter-cell morphology in P6–8 hGFAP-CreER;Ai14 transgenic mice and found the two daughter cells occupying comparable areas and showing similar labelling with the astrocyte marker, BLBP (Fig. 4d and Supplementary Table 1). Thus, locally dividing astrocytes in the cortex primarily undergo symmetrical division to generate two daughter astrocytes.

To determine whether the progeny maintained their astrocytic fate after exiting from the cell cycle, we administered tamoxifen at P0–2 to hGFAP-CreER;Ai14 transgenic mice to label astrocytes permanently with tdTomato and examined their locally generated progeny 1 week later ($n = 4$ mice) to test whether these tdTomato$^+$ cells still expressed the astrocyte marker BLBP. Although there were many progenitors or neurons with tdTomato expression in SVZ and hippocampal dentate gyrus (Supplementary Fig. 7f, g), nearly all of the tdTomato$^+$ cells were BLBP$^+$ or GFAP$^+$ in the cortex (99.8%, motor and barrel cortex; Supplementary Fig. 7a–e). Because we found that few astrocytes would enter programmed cell death in the cortex (Supplementary Fig. 13), it is most likely that the progeny arising from local astrocyte division retained astrocytic identity long after exiting from the cell cycle. For
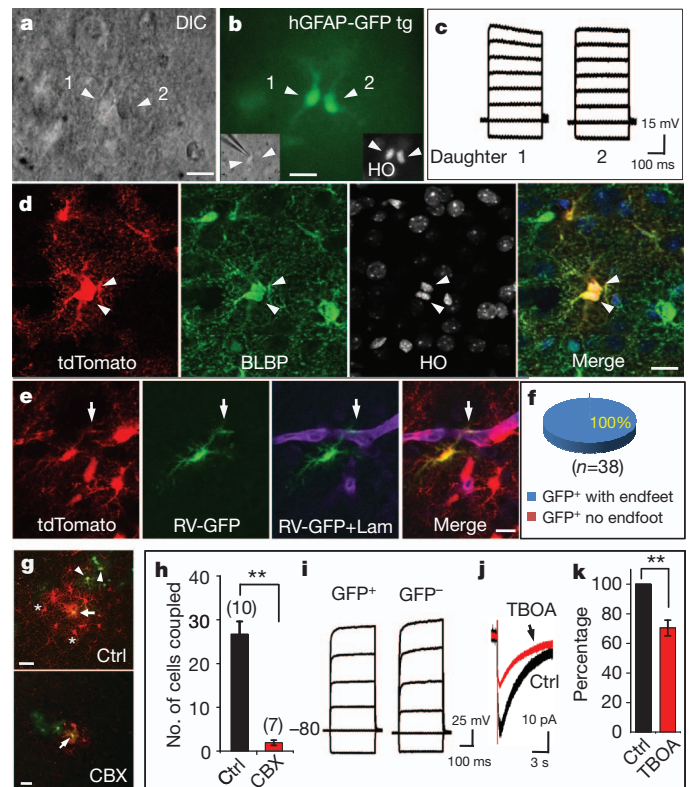
Figure 4 | Symmetric division of proliferating astrocytes and the function of their progeny. a, A pair of daughter astrocytes (arrowheads) at late telophase under differential interference contrast. **b**, Both cells had GFP signal. Nuclei were stained with Hoechst 33342 (HO, inset). **c**, Voltage responses of two daughter cells evoked by step currents (−1 to 6 nA). **d**, Two daughter cells in telophase (arrowheads) from a P8 hGFAP-CreER;Ai14 transgenic mouse. **e**, An astrocyte infected by GFP-expressing retroviruses (green) and expressing tdTomato (red) formed endfeet (arrows) with blood vessels (Laminin$^+$, purple) in a P19 hGFAP-CreER;Ai14 transgenic mouse. Tamoxifen was injected at P2, and cells were infected with retrovirus at P5. **f**, The percentage of progeny cells marked by retroviruses (GFP$^+$tdTomato$^+$) that had endfeet (GFP$^+$tdTomato$^+$ with endfeet, blue). **g**, A retrovirus-infected astrocyte progeny (GFP$^+$, green, arrow) in the absence (Ctrl, upper) or presence (lower) of 100 μM carbenoxolene (CBX) was injected with biocytin (red). Without CBX, both GFP$^+$ astrocytes (arrowheads) and GFP$^-$ astrocytes (asterisks) contained biocytin (red), as a result of gap-junction coupling with the astrocyte progeny injected with biocytin. **h**, The number of cells coupled. Two asterisks, $P < 0.01$, (unpaired t-test). **i**, Current responses of uninfected (GFP$^-$) and infected (GFP$^+$) astrocyte progeny. **j, k**, Glutamate transporter current (**j**) and its summarized data (**k**) from infected astrocyte progeny before (black) and after (red) application of blocker TBOA (100 μM, $70.4 \pm 5.3\%$, $n = 7$). Two asterisks, $P < 0.01$ (paired t-test). Scale bars, 10 μm (**a, b, d, e**) and 20 μm (**g**). Error bars indicate s.e.m.

further confirmation, tamoxifen was administered at P0–2 and retroviruses were injected locally at P3–5 (3 days after tamoxifen) in the cortex of hGFAP-CreER;Ai14 transgenic mice. The fate of doubly labelled cells (tdTomato$^+$GFP$^+$) was then assessed 2 weeks later. Because tdTomato marked cells that had expressed astrocyte markers before retroviral infection (Supplementary Fig. 7), the tdTomato$^+$GFP$^+$ cells correspond to the progeny of astrocytes that were infected by retroviruses during cell division. We found that all doubly labelled cells formed endfoot-like structures with blood vessels (38 of 38 yellow cells; Fig. 4e, f), a characteristic of differentiated astrocytes. These results demonstrate that locally generated progeny retain astrocytic identity long after they exit from the cell cycle.

We then asked whether daughter astrocytes arising from local astrocyte division integrate functionally into the existing glial network as mature astrocytes. The intercellular communication by means of gap junctions between astrocytes has a critical function in ion buffering

in the brain[26]. At 1–3 weeks after viral infection, we loaded biocytin into infected astrocytes and found that biocytin diffused into neighbouring GFP$^-$ astrocytes as well as some GFP$^+$ astrocytes within 20 min (26.7 ± 2.9 cells, $n = 10$ slices; Fig. 4g–i and Supplementary Fig. 14). The coupling was inhibited by carbonoxelene (CBX), a blocker for gap junctions (1.9 ± 0.6 cells, $n = 7$ slices; Fig. 4g, h and Supplementary Fig. 14), indicating that locally generated astrocytes successfully integrated into existing glial networks. Another classical function of astrocytes is to clear glutamate from the synaptic cleft[27]. After stimulation of neuronal fibres, an inward current with slow decay time course appeared in all the GFP$^+$ astrocytes recorded (20 of 20 GFP$^+$ cells, P12–19; Fig. 4j) and was sensitive to the glutamate transporter blocker TBOA (Fig. 4j, k). The remaining currents, lasting for more than 10 s (decay time 13.3 ± 0.4 s, $n = 4$; Fig. 4j), correspond to K_{ir} activation after neuronal excitation[28]. These observations thus reveal that locally generated astrocytes function as mature astrocytes to take up glutamate and K^+ ions after neuronal activity.

We have demonstrated that local generation of astrocytes within the postnatal cortex provides a major glial source, at least in layers I–IV, whereas astrocytes generated early in development are derived from radial glia[4–6], SVZ progenitors (including SVZ glioblasts and migratory glioblasts)[4–6,20]. Once a subset of early astrocytes from those sources colonize and differentiate in the cortex as 'pioneers', local division of these differentiated astrocytes has a pivotal role in glial production after birth in the cortex.

Astrocytic endfeet almost fully cover the blood vessels by postnatal day 20 and are crucial to the regulation of cerebral blood flow[29] and the transport of nutrients from blood to neurons[30]. It is not yet clear how this large number of locally generated astrocytes can coordinate with angiogenesis to form the complete gliovascular interface. Furthermore, aberrant gene activity affecting glial proliferation is one potential cause of gliomas, which comprise nearly 80% of primary malignant brain tumours[3]. It will also be of interest to test whether gliomas could have arisen from defective regulation of locally dividing glial cells in the brain.

METHODS SUMMARY

For live nuclear labelling, slices were incubated with Hoechst 33342 (2 μg ml^{-1}) as described previously[14]. For in vivo imaging, the pups with thinned skull (Fig. 3h, l, m) were immobilized with 4% agarose. The mouth of the pup was attached to a 1-ml pipette tip that was connected to a tube for inhalation. All data are given as means ± s.e.m.

Full Methods and any associated references are available in the online version of the paper at www.nature.com/nature.

1. Azevedo, F. A. et al. Equal numbers of neuronal and nonneuronal cells make the human brain an isometrically scaled-up primate brain. J. Comp. Neurol. **513**, 532–541 (2009).
2. Eroglu, C. & Barres, B. A. Regulation of synaptic connectivity by glia. Nature **468**, 223–231 (2010).
3. Schwartzbaum, J. A., Fisher, J. L., Aldape, K. D. & Wrensch, M. Epidemiology and molecular pathology of glioma. Nat. Clin. Pract. Neurol. **2**, 494–503 (2006).
4. Cameron, R. S. & Rakic, P. Glial cell lineage in the cerebral cortex: a review and synthesis. Glia **4**, 124–137 (1991).
5. Marshall, C. A., Suzuki, S. O. & Goldman, J. E. Gliogenic and neurogenic progenitors of the subventricular zone: who are they, where did they come from, and where are they going? Glia **43**, 52–61 (2003).
6. Kriegstein, A. & Alvarez-Buylla, A. The glial nature of embryonic and adult neural stem cells. Annu. Rev. Neurosci. **32**, 149–184 (2009).
7. Bandeira, F., Lent, R. & Herculano-Houzel, S. Changing numbers of neuronal and non-neuronal cells underlie postnatal brain growth in the rat. Proc. Natl Acad. Sci. USA **106**, 14108–14113 (2009).
8. Levison, S. W. & Goldman, J. E. Both oligodendrocytes and astrocytes develop from progenitors in the subventricular zone of postnatal rat forebrain. Neuron **10**, 201–212 (1993).
9. Zerlin, M., Levison, S. W. & Goldman, J. E. Early patterns of migration, morphogenesis, and intermediate filament expression of subventricular zone cells in the postnatal rat forebrain. J. Neurosci. **15**, 7238–7249 (1995).
10. Smart, I. & Leblond, C. P. Evidence for division and transformations of neuroglia cells in the mouse brain, as derived from radioautography after injection of thymidine-H^3. J. Comp. Neurol. **116**, 349–367 (1961).
11. Suh, H. et al. In vivo fate analysis reveals the multipotent and self-renewal capacities of Sox2$^+$ neural stem cells in the adult hippocampus. Cell Stem Cell **1**, 515–528 (2007).
12. Guo, F., Ma, J., McCauley, E., Bannerman, P. & Pleasure, D. Early postnatal proteolipid promoter-expressing progenitors produce multilineage cells in vivo. J. Neurosci. **29**, 7256–7270 (2009).
13. Sakaue-Sawano, A. et al. Visualizing spatiotemporal dynamics of multicellular cell-cycle progression. Cell **132**, 487–498 (2008).
14. Ge, W. P., Zhou, W., Luo, Q., Jan, L. Y. & Jan, Y. N. Dividing glial cells maintain differentiated properties including complex morphology and functional synapses. Proc. Natl Acad. Sci. USA **106**, 328–333 (2009).
15. Ge, W. P. et al. Long-term potentiation of neuron-glia synapses mediated by Ca^{2+}-permeable AMPA receptors. Science **312**, 1533–1537 (2006).
16. Wang, D. D., Krueger, D. D. & Bordey, A. Biophysical properties and ionic signature of neuronal progenitors of the postnatal subventricular zone in situ. J. Neurophysiol. **90**, 2291–2302 (2003).
17. Madisen, L. et al. A robust and high-throughput Cre reporting and characterization system for the whole mouse brain. Nature Neurosci. **13**, 133–140 (2010).
18. Casper, K. B., Jones, K. & McCarthy, K. D. Characterization of astrocyte-specific conditional knockouts. Genesis **45**, 292–299 (2007).
19. Zhuo, L. et al. Live astrocytes visualized by green fluorescent protein in transgenic mice. Dev. Biol. **187**, 36–42 (1997).
20. Burns, K. A., Murphy, B., Danzer, S. C. & Kuan, C. Y. Developmental and post-injury cortical gliogenesis: a genetic fate-mapping study with Nestin-CreER mice. Glia **57**, 1115–1129 (2009).
21. Zhu, X. et al. Age-dependent fate and lineage restriction of single NG2 cells. Development **138**, 745–753 (2011).
22. Matthias, K. et al. Segregated expression of AMPA-type glutamate receptors and glutamate transporters defines distinct astrocyte populations in the mouse hippocampus. J. Neurosci. **23**, 1750–1758 (2003).
23. Buffo, A. et al. Origin and progeny of reactive gliosis: a source of multipotent cells in the injured brain. Proc. Natl Acad. Sci. USA **105**, 3581–3586 (2008).
24. Xu, H. T., Pan, F., Yang, G. & Gan, W. B. Choice of cranial window type for in vivo imaging affects dendritic spine turnover in the cortex. Nature Neurosci. **10**, 549–551 (2007).
25. Doetsch, F., Caille, I., Lim, D. A., Garcia-Verdugo, J. M. & Alvarez-Buylla, A. Subventricular zone astrocytes are neural stem cells in the adult mammalian brain. Cell **97**, 703–716 (1999).
26. Gutnick, M. J., Connors, B. W. & Ransom, B. R. Dye-coupling between glial cells in the guinea pig neocortical slice. Brain Res. **213**, 486–492 (1981).
27. Bergles, D. E. & Jahr, C. E. Synaptic activation of glutamate transporters in hippocampal astrocytes. Neuron **19**, 1297–1308 (1997).
28. Ge, W. P. & Duan, S. Persistent enhancement of neuron-glia signaling mediated by increased extracellular K$^+$ accompanying long-term synaptic potentiation. J. Neurophysiol. **97**, 2564–2569 (2007).
29. Takano, T. et al. Astrocyte-mediated control of cerebral blood flow. Nature Neurosci. **9**, 260–267 (2006).
30. Rouach, N., Koulakoff, A., Abudara, V., Willecke, K. & Giaume, C. Astroglial metabolic networks sustain hippocampal synaptic transmission. Science **322**, 1551–1555 (2008).

Author Contributions W.-P.G. conceived the project, designed and performed the experiments and analysed the data. L.Y.J. and Y.N.J. supervised the work and helped to design the experiments. W.-P.G. and L.Y.J. wrote the manuscript. F.H.G. and A.M. provided MLV retrovirus and CAG-Fucci-Green transgenic mice, respectively. All authors reviewed and edited the manuscript.

Author Information Reprints and permissions information is available at www.nature.com/reprints. The authors declare no competing financial interests. Readers are welcome to comment on the online version of this article at www.nature.com/nature. Correspondence and requests for materials should be addressed to L.Y.J. (lily.jan@ucsf.edu).

METHODS

Animals and tamoxifen administration. The CAG-Fucci-Green transgenic line was from A.M.'s laboratory, the hGFAP-CreER line was from K. D. McCarthy's laboratory (UNC), and the NG2BacDsRed transgenic line was from A. Nishiyama's laboratory. Both NG2-CreBac[31] and NG2-CreER were generated in Nishiyama's laboratory and bought from Jackson Laboratory. The Ai14 transgenic mice was from H. Zeng's laboratory. Tamoxifen inductions were as described[18]. For induction in hGFAP-CreER;Ai14 transgenic mice, an intraperitoneal or subcutaneous injection of tamoxifen (dissolved in a 1:10 mixture of ethanol and sunflower oil) at 3 mg per 40 g of body weight was administered once at the time indicated. All animals were treated in accordance with protocols approved by the Institutional Animal Care and Use Committee at UCSF.

In vivo **electroporation.** Newborn to 2-day-old pups (P0–2) were anaesthetized by hypothermia (about 4 min) and fixed to a support with a sticking plaster. GFP complementary DNAs were cloned into the chicken β-actin CMV promoter-driven expression vector pCAGGS. DNA solution (1–2 μl) prepared at 2 mg ml^{-1} in 10 mM Tris-HCl pH 8.0, with 0.04% trypan blue, was injected into the lateral ventricle with a pulled-out glass capillary (diameter 50–100 μm)[32]. Animals were subjected to five electric stimuli of 50 V, each lasting 50 ms, at 950-ms intervals using a square-pulse electroporator BTX830.

Retroviral preparation and *in vivo* **infection.** pCAG-GFP-PRE contains replication-defective murine leukaemia virus (MLV)-based retroviral elements designed to carry and express enhanced GFP under CMV promoter and CAG promoter (modified chicken β-actin promoter with enhanced sequences from CMV) with control of the MLV long terminal repeat. We followed the detailed protocol for preparation from Gage's laboratory[33]. In brief, three plasmids (pCAG-GFP-PRE, pCMV-gp and CMV-vsvg) were transfected to HEK 293T cells with Lipofectamine 2000. Viruses containing supernatants were harvested 2 days after transfection by centrifugation twice at 65,000g for 2 h (Discovery 90SE; Sorvall). Final virus titres were about 10^6–10^7 colony-forming units ml^{-1} as measured by infecting HEK 293T cells. Viruses with the GFP reporter gene were injected (1 μl) into either C57BL/6 wild-type or hGFAPCreER;Ai14 transgenic mice at P0–9. For *in vivo* infection, pups were anaesthetized with ice for 3–5 min, and the injection was performed as described[34]. After injection, the pups were put back in a cage with a lamp to keep them warm. They were returned to their home cage when fully recovered.

Immunocytochemistry. Mice were perfused with 4% paraformaldehyde in 1 × PBS. Brains were cut into sections 25–50 μm thick with a cryostat (model CM3050S; Leica). Floating sections were permeabilized with 0.25% Triton X-100 in 1 × PBS and then blocked for 2 h with 5% BSA and 3% normal goat serum with 0.25% Triton X-100 in 1 × PBS. Primary antibodies for Ki67 (1:200 dilution, rabbit, monoclonal; Thermo Scientific), BLBP (1:1,000, rabbit, polyclonal; Invitrogen) or Laminin (1:500, rabbit, polyclonal; Sigma) were applied to sections alone or in combination and left to incubate for 24–48 h at 4 °C. Together with DAPI or Hoechst 33342 (1 μg ml^{-1}; Invitrogen), secondary antibodies conjugated with Alexa488, 555, 568 or 633 (1:750) were applied for 2 h at room temperature (22–25 °C). To identify apoptotic astrocytes, sections were incubated for 15 min with 1 μg ml^{-1} propidium iodide after the treatment with 0.2 mg ml^{-1} RNase (DNase-free) in 1 × PBS for 30 min at 37 °C as described previously[35,36].

Slice preparation. Slices were prepared as described previously[15]. In brief, after decapitation, mouse brains were dissected rapidly and sliced with a vibratome (VT-1000S; Leica) in ice-cold oxygenated (95% O$_2$ and 5% CO$_2$) artificial cerebrospinal fluid solution (aCSF) containing (in mM): 119 NaCl, 2.5 KCl, 2.5 CaCl$_2$, 1.3 MgSO$_4$, 1 NaH$_2$PO$_4$, 26.2 NaHCO$_3$ and 11 glucose. Transverse slices (250 μm in thickness) were then maintained in an incubation chamber for at least 1 h at room temperature before whole-cell recording, nuclear dye loading or time-lapse imaging.

Electrophysiology and live cell nuclear labelling. Whole-cell recordings from mouse brain slices were conducted with the aid of markers (GFP or Hoechst 33342) to identify infected cells or dividing cells. Astrocytes in hGFAP-GFP transgenic mice were identified by bright green fluorescence under the microscope. For live nuclear labelling, slices were incubated with Hoechst 33342 (diluted to 2 μg ml^{-1} in aCSF) at room temperature for 30 min as described previously[14]. Recording pipettes were routinely filled with a solution containing (in mM): 125 potassium gluconate, 15 KCl, 10 HEPES, 3 MgATP, 0.3 Na-GTP, 5 Na-phosphocreatine and 0.2 EGTA (pH 7.2–7.4, 290–300 mosM). For glutamate transporter currents, pipette solution contained (in mM): 125 caesium gluconate, 5 CsCl, 10 HEPES, 3 MgATP, 0.3 Na-GTP, 0.2 EGTA and 5 Na-phosphocreatine (pH 7.2–7.4, 290–300 mosM). Membrane potential in voltage-clamp mode was held at −80 mV. Current pulses (20–60 μA, 0.1 ms, 0.05 Hz) were delivered through extracellular bipolar electrodes placed roughly 200–300 μm from the cells being recorded to induce transporter current.

Biocytin labelling. Glial cells were filled with 0.1% biocytin (ε^N-biotinyl-L-lysine; Vector Lab) by means of a whole-cell recording electrode, as reported previously[15,28]. Biocytin was dissolved in the recording pipette solution. Slices were fixed overnight with 4% paraformaldehyde at 4 °C before treatment for 2 h with blocking solution containing 5% BSA, 3% normal goat serum and 0.25% Triton X-100. Slices were then stained for 2 h with DyLight 549-conjugated streptavidin (1:1,000; Vector Lab). In Fig. 2o, DyLight 549 was added together with Alexa 633 (second antibodies against anti-Ki67) after washing out excess primary antibody against Ki67.

Confocal time-lapse imaging of acute brain slices. GFP$^+$ cells at cortical slices from hGFAP-GFP transgenic mice (P3–5) were imaged on a Zeiss LSM510 two-photon confocal microscope equipped with objective 20×/0.5W and 63×/0.9W (Zeiss). Cells were scanned with *xyz* mode (four optical slices in *z*, with 8-μm interval between slices). The frame interval was 4 min for 30–100 frames. Projection images were made from *z*-stacks that included all individual GFP$^+$ cells. During imaging, slices were kept in a chamber with perfusion of aCSF (see above) at 32–34 °C.

Confocal time-lapse imaging *in vivo***.** The pups (P3–6, hGFAP-CreER;Ai14 transgenic pups; Fig. 3l, m) were anaesthetized by hypothermia: 4–5 min in ice wrapped in a piece of cloth. A small fraction of skin (3 mm × 3 mm) was removed over an area to be imaged. The pups then were returned to a box for 3–4 h until the incision site healed (no bleeding). A high-speed micro-drill was used to thin a circular area of skull, typically about 1 mm in diameter. The mouth of the pup was attached to a 1-ml pipette tip that was connected to a tube for inhalation. Pups were then immobilized with 4% agarose. Imaging was performed using a two-photon laser-scanning microscope based on a mode-locked laser system operating at 930 nm, equipped with one of the following objectives: 10×, 0.25 numerical aperture (NA); 20×, 0.8 NA collected emission more than 560 nm for tdTomato and 500–550 nm for mAG. Sometimes tdTomato was excited with a laser at 543 nm. Images were taken every 1.5 h for the first 3 h, and then the pups were put back in a box and allowed to move freely. Additional images were taken every 9–12 h for the following 18–24 h. During imaging, pups were fully anaesthetized with 2–4% isoflurane for 4–5 min. Cells under the pia were scanned with *xyz* mode (16 slices in *z* with 10-μm interval between optical slices.). Shortly after an imaging session, isoflurane was turned off and oxygen was left on until the animal fully recovered. For Fucci-Green;hGFAP-CreER;Ai14 pups (Fig. 3i–k) we removed a small fraction of the skull (1 mm^2) and images were taken within 1 h after surgery.

31. Zhu, X., Bergles, D. E. & Nishiyama, A. NG2 cells generate both oligodendrocytes and gray matter astrocytes. *Development* **135,** 145–157 (2008).
32. Li, G. *et al.* Regional distribution of cortical interneurons and development of inhibitory tone are regulated by Cxcl12/Cxcr4 signaling. *J. Neurosci.* **28,** 1085–1098 (2008).
33. Tashiro, A., Zhao, C. & Gage, F. H. Retrovirus-mediated single-cell gene knockout technique in adult newborn neurons *in vivo*. *Nature Protocols* **1,** 3049–3055 (2006).
34. Merkle, F. T., Mirzadeh, Z. & Alvarez-Buylla, A. Mosaic organization of neural stem cells in the adult brain. *Science* **317,** 381–384 (2007).
35. Barres, B. A. *et al.* Cell death and control of cell survival in the oligodendrocyte lineage. *Cell* **70,** 31–46 (1992).
36. Krueger, B. K., Burne, J. F. & Raff, M. C. Evidence for large-scale astrocyte death in the developing cerebellum. *J. Neurosci.* **15,** 3366–3374 (1995).